Junctate boosts phagocytosis by recruiting endoplasmic reticulum Ca2+ stores near phagosomes

Guido, Danièle; Demaurex, Nicolas; Nunes-Hasler, Paula

How to cite

GUIDO, Danièle, DEMAUREX, Nicolas, NUNES-HASLER, Paula. Junctate boosts phagocytosis by recruiting endoplasmic reticulum Ca2+ stores near phagosomes. In: Journal of cell science, 2015, vol. 128, n° 22, p. 4074–4082. doi: 10.1242/jcs.172510

This publication URL: https://archive-ouverte.unige.ch/unige:88513
Publication DOI: 10.1242/jcs.172510

© 2015. Published by The Company of Biologists Ltd | Journal of Cell Science (2015) 128, 4074-4082 doi:10.1242/jcs.172510

RESEARCH ARTICLE

Junctate boosts phagocytosis by recruiting endoplasmic reticulum Ca^{2+} stores near phagosomes

Daniele Guido, Nicolas Demaurex* and Paula Nunes*

ABSTRACT

Local intracellular Ca^{2+} elevations increase the efficiency of phagocytosis, a process that is essential for innate and adaptive immunity. These local Ca^{2+} elevations are generated in part by the store-operated Ca^{2+} entry (SOCE) sensor STIM1, which recruits endoplasmic reticulum (ER) cisternae to phagosomes and opens phagosomal Ca^{2+} channels at ER–phagosome junctions. However, residual ER–phagosome contacts and periphagosomal Ca^{2+} hotspots remain in *Stim1*$^{-/-}$ cells. Here, we tested whether junctate (also called ASPH isoform 8), a molecule that targets STIM1 to ER–plasma-membrane contacts upon Ca^{2+}-store depletion, cooperates with STIM1 at phagosome junctions. Junctate expression in *Stim1*$^{-/-}$ and *Stim1*$^{-/-}$*; Stim2*$^{-/-}$ phagocytic fibroblasts increased phagocytosis and periphagosomal Ca^{2+} elevations, yet with only a minimal impact on global SOCE. These Ca^{2+} hotspots were only marginally reduced by the SOCE channel blocker lanthanum chloride (La^{3+}) but were abrogated by inositol trisphosphate receptor inhibitors 2-APB and xestospongin-C, revealing that unlike STIM1-mediated hotspots, junctate-mediated Ca^{2+} originates predominantly from periphagosomal Ca^{2+} stores. Accordingly, junctate accumulates near phagosomes and elongates ER–phagosome junctions in *Stim1*$^{-/-}$ cells. Thus, junctate mediates an alternative mechanism for generating localized Ca^{2+} elevations within cells, promoting Ca^{2+} release from internal stores recruited to phagosomes, thereby boosting phagocytosis.

KEY WORDS: Ca^{2+}, Capacitive calcium entry, Ion channel, Junctate, Signal transduction, Membrane contact site, Phagocytosis

INTRODUCTION

Phagocytosis, the engulfment of foreign particles into a membrane-enclosed vacuole known as the phagosome, is a fundamental cellular process that is essential for bacterial killing and antigen presentation by innate immune cells. The phagocytic process comprises two phases, an ingestion phase that is characterized by the recognition of the particle and its actin-driven engulfment into a new membrane-derived organelle, as well as a maturation phase during which the phagosome acquires oxidative and lytic properties through fusion with endosomes and lysosomes (Aderem and Underhill, 1999). The kinetics and efficiency of phagosome maturation is promoted by both global as well as localized Ca^{2+} elevations occurring during phagocytosis that drive the shedding of the actin coat (Bengtsson et al., 1993), the assembly and activation of the phagocytic NAPDH oxidase (Dewitt et al., 2003), and the fusion with lysosomes (Jaconi et al., 1990), reviewed by Nunes and Demaurex (2010). Global Ca^{2+} elevations occur during phagocytosis as a result of phagocytic receptor ligation and phospholipase-C- or phospholipase-D-driven store-operated Ca^{2+} entry (SOCE) (Nunes and Demaurex, 2010). Localized periphagosomal Ca^{2+} elevations can be generated in two ways – either by the opening of Ca^{2+} release channels on intracellular Ca^{2+} stores located in the vicinity of phagosomes or by the opening of Ca^{2+} channels present on phagosomes through mechanisms that have only recently begun to be uncovered. We have previously shown that the transmembrane endoplasmic reticulum (ER) Ca^{2+} sensor stromal interaction molecule 1 (STIM1) recruits ER cisternae to phagosomes and promotes the opening of phagosomal Ca^{2+} channels (Nunes et al., 2012). STIM1 mediates the ubiquitous SOCE mechanism (Liou et al., 2005; Roos et al., 2005; Zhang et al., 2005) by acting as an intracellular ligand for plasma membrane Ca^{2+}-permeable channels of the Orai (Feske et al., 2006; Vig et al., 2006; Zhang et al., 2006) and transient receptor potential canonical (TRPC) families (Huang et al., 2006; reviewed in Hogan et al., 2010), together referred to as store-operated Ca^{2+} (SOCE) channels. Upon ER Ca^{2+} depletion, STIM1 oligomerizes and accumulates in cortical contact sites between the ER and plasma membrane (Luik et al., 2008; Lur et al., 2009; Orci et al., 2009; Wu et al., 2006), where its channel activating domain (CAD) directly interacts with Orai1 to promote channel opening (Luik et al., 2006; Park et al., 2009; Xu et al., 2006; Zhou et al., 2010). Three independent synergistic mechanisms promote STIM1 localization at ER–plasma-membrane junctions: (1) STIM1 binding to phosphoinositides through the exposed polylysine C-terminal tail (Walsh et al., 2010), (2) binding of the STIM1 cytoplasmic CAD domain to Orai1 (Huang et al., 2006; Muik et al., 2009; Park et al., 2009; Yuan et al., 2009), and (3) Ca^{2+}-regulated binding of STIM1 through its luminal domain to junctate (Srikanth et al., 2012)].

Junctate is a ubiquitously expressed 33-kDa single-pass transmembrane ER protein bearing a luminal EF-hand motif, generated by alternative splicing of the gene encoding junctin and aspartate-β-hydroxylase (*ASPH* isoform 8) (Dinchuk et al., 2000; Hong et al., 2001; Treves et al., 2000). Junctate and STIM1 interact through their luminal domains, thereby facilitating STIM1 recruitment to membrane contact sites (Srikanth et al., 2012), and interacts with the inositol 1,4,5 trisphosphate receptor (InsP3R) and with TRPC channels through its cytosolic N-terminus (Treves et al., 2004, 2010). Junctate also interacts with sarco-endoplasmic reticulum Ca^{2+} ATPase 2a (SERCA2a) in cardiomyocytes to regulate sarcoplasmic reticulum Ca^{2+} cycling (Kwon and Kim, 2009), and mice overexpressing junctate develop myocardial hypertrophy (Hong et al., 2008), highlighting the importance of junctate in Ca^{2+} homeostasis. Junctate populates plasma membrane clusters in resting cells, indicating that it is a structural component of ER–plasma-membrane contact sites, and junctate overexpression

Department of Cell Physiology and Metabolism, University of Geneva, 1 rue Michel-Servet, Geneva 4 CH-1211, Switzerland.

*Authors for correspondence (Nicolas.Demaurex@unige.ch; Paula.Nunes@unige.ch)

Received 2 April 2015; Accepted 2 October 2015

Journal of Cell Science

Journal of Cell Science (2015) 128, 4074-4082 doi:10.1242/jcs.172510

elongates and stabilizes ER–plasma–membrane junctions and increases the amount of Ca^{2+} released from intracellular Ca^{2+} stores (Treves et al., 2004, 2010). The N-terminus of junctate is devoid of lipid-binding motifs but is required for junctate accumulation in plasma membrane clusters, suggesting that junctate provides an alternative mechanism of STIM1 recruitment that is independent of phosphoinositides and Orai1(Srikanth et al., 2012). Such a mechanism might be important for the targeting of STIM1 to membranes that have distinct phosphoinositide compositions, or importantly, for the delivery of Ca^{2+} stores to target membranes independently of STIM1.

Phagosomes, although derived from the plasma membrane, have a very distinct lipid and protein composition because extensive sorting occurs during phagosome engulfment. In a previous study, we detected a significant number of ER–phagosome junctions, as well as residual Ca^{2+} hotspots (also called microdomains), in primary neutrophils as well as in mouse embryonic fibroblasts (MEFs) that had been engineered to be phagocytic and isolated from mice in which STIM1 had been genetically ablated. These results suggest that proteins other than STIM1 recruit ER cisternae and mediate localized Ca^{2+} signaling near phagosomes. We therefore postulated that junctate cooperates with STIM1 to recruit ER cisternae to phagosomes, thereby providing an alternative mechanism for generating periphagosomal Ca^{2+} hotspots. We tested this hypothesis by expressing junctate in fibroblasts, which had been rendered phagocytic through expression of FcγRIIA receptors (also known as FCGR2A), from STIM1-knockout mice. Our data show that junctate recruits ER Ca^{2+} stores to phagosomes and promotes localized Ca^{2+} elevations that sustain high-efficiency phagocytosis.

RESULTS

Junctate is recruited to phagosomes independently of STIM1

To assess whether junctate is recruited to phagosomes, we quantified the percentage of phagosomes that were decorated by yellow fluorescent protein (YFP)–junctate, by green fluorescent protein (GFP)–KDEL as a control ER marker, or by mCherry–STIM1, which we have previously shown to be recruited to phagosomes (Nunes et al., 2012). The proteins were expressed in wild-type, *Stim1*$^{-/-}$ and *Stim1*$^{-/-}$; *Stim2*$^{-/-}$ MEFs that had been rendered phagocytic through co-expression with FcγRIIA–c-Myc receptors, and cells were then exposed to IgG-opsonized red blood cells (RBCs). To synchronize phagocytosis, RBCs were centrifuged onto cells that had been seeded on coverslips, and cells were allowed to phagocytose for 10 min before fixation. Coverslips were then immunostained to reveal c-Myc tagged Fc receptors, and imaged by using confocal microscopy. Quantification through visual inspection of confocal *z*-stacks revealed that both GFP–KDEL and YFP–junctate fluorescent clusters (or puncta) were observed around ∼40% of phagosomes found in wild-type cells (Fig. 1A). In *Stim1*$^{-/-}$ cells, no discernible periphagosomal GFP–KDEL clusters could be detected, whereas YFP–junctate and mCherry–STIM1 clusters decorated 31% and 57% of phagosomes, respectively (Fig. 1B). When the proteins were expressed in *Stim1*$^{-/-}$; *Stim2*$^{-/-}$ cells, YFP–junctate and mCherry–STIM1 clusters decorated 57% and 68% of phagosomes compared with 16% of phagosomes for GFP–KDEL (Fig. 1C). The absence of GFP–KDEL clusters in *Stim1*$^{-/-}$ but not *Stim1*$^{-/-}$; *Stim2*$^{-/-}$ cells might reflect the difficulty to identify clusters owing to the low and more finely reticular expression pattern of the ER marker in *Stim1*$^{-/-}$ cells (compare

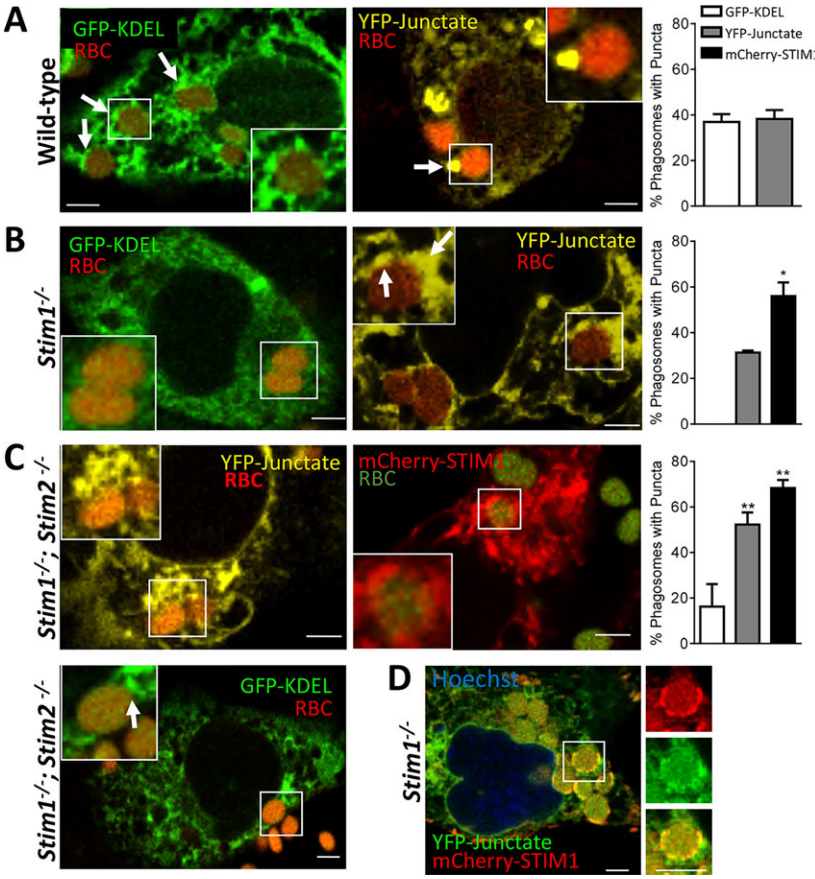

Fig. 1. Junctate is recruited to phagosomes in a STIM1-independent manner. (A) Three-dimensional projections of confocal *z*-stacks show that in wild-type MEFs, GFP–KDEL puncta (left panel, green), as well as YFP–junctate puncta (middle panel, yellow) are observed near red blood cell (RBC)-containing phagosomes (red) at similar frequencies (right panel). Arrows indicate periphagosomal puncta. (B) Contrary to wild-type MEFs, GFP–KDEL puncta (left panel, green) are not detectable around phagosomes in *Stim1*$^{-/-}$ MEFs. In contrast, YFP–junctate (middle panel, yellow) still localized near to phagosomes in the absence of STIM1, albeit at a lower frequency than mCherry–STIM1 puncta (right panel). (C) YFP–junctate (upper left panel, yellow) and mCherry–STIM1 (middle panel, red) are recruited to phagosomes (red in left panel, green in middle panel) in *Stim1*$^{-/-}$; *Stim2*$^{-/-}$ MEFs at 3- to 3.5-fold higher frequencies (right panel) than GFP–KDEL (green, lower left panel). (D) YFP–junctate (green) and mCherry–STIM1 (red) colocalize in periphagosomal puncta when co-expressed in *Stim1*$^{-/-}$ MEFs. Scale bars: 3 µm. Data are means±s.e.m. of three independent experiments, comprising the following number of cells, phagosomes, puncta. Wild type: KDEL, 121, 247, 92; junctate, 155, 150, 63. *Stim1*$^{-/-}$: KDEL, 189, 271, 0; junctate, 193, 404, 127; STIM1, 154, 242, 129. *Stim1*$^{-/-}$; *Stim2*$^{-/-}$: KDEL, 99, 36, 11; junctate, 91, 83, 45; STIM1, 95, 119, 82.*P<0.05, **P<0.01, ***P<0.001.

Journal of Cell Science (2015) 128, 4074-4082 doi:10.1242/jcs.172510

Fig. 1B left panel and Fig. 1C lower left panel). Alternatively, an altered nature of residual contact sites in cells expressing only STIM2 could account for this difference. Interestingly, when co-expressed in *Stim1*$^{-/-}$ MEFs, YFP–junctate and STIM1–mCherry both localized in the same periphagosomal clusters (Fig. 1D). These data indicate that junctate is recruited to phagosomes independently of STIM proteins but might interact with STIM1 at ER–phagosome contact sites.

Junctate expression increases the size of phagosome–ER junctions

To establish whether junctate recruits ER cisternae to the vicinity of phagosomes and/or alters the morphology of ER–phagosome-membrane contact sites, we quantified the extent of ER cisternae recruitment to phagosomes by using electron microscopy in 50-nm slices. To normalize for the cross-sectional sampling, junctional ER was quantified as the average contact length divided by the perimeter of the phagosome (Fig. 2, arrows). Contacts were defined as the contiguous length of an ER cisterna that discernibly remained ≤30 nm from the membrane of a phagosome. These juxtaposed ER structures were detected in 23–29% of phagosomes forming in *Stim1*$^{-/-}$ and wild-type phagocytic MEFs, regardless of junctate expression (Fig. 2), and the length of the recruited ER structures averaged ∼250 nm (268±51 nm for YFP–junctate and 231±58 nm for GFP–KDEL, corresponding to 2.84±0.54% and 2.45±0.62% of the phagosome perimeter, n=20 and 28, respectively; mean±s.e.m.; Fig. 2). By contrast, YFP–junctate expression doubled the length of the recruited cisternae in *Stim1*$^{-/-}$ cells (231±36 nm vs 115±19 nm for GFP–KDEL, corresponding to 2.45±0.38% vs 1.22±0.20% of the phagosome perimeter, n=24 for each; Fig. 2). Qualitative differences were also apparent as the juxtaposed ER cisternae were thinner in *Stim1*$^{-/-}$ cells expressing YFP–junctate (Fig. 2, arrows). These data indicate that junctate, when expressed in the absence of STIM1, can promote the elongation of periphagosomal ER cisternae.

Junctate mediates store-operated Ca^{2+} entry in the absence of STIM proteins

Junctate has been previously reported to populate STIM1–Orai1 membrane contact sites and to interact with TRPC channels, suggesting that this protein might modulate the activity of Ca^{2+} entry channels. To test this hypothesis, we measured Ca^{2+} entry rates following store depletion with the SERCA inhibitor thapsigargin in cells expressing either YFP–junctate, GFP–KDEL or mCherry–STIM1 as controls. Junctate expression had no impact on Ca^{2+} entry rates in wild-type or *Stim1*$^{-/-}$ MEFs, but surprisingly, junctate increased Ca^{2+} entry rates in *Stim1*$^{-/-}$; *Stim2*$^{-/-}$ MEFs by twofold. In comparison, STIM1 re-expression in *Stim1*$^{-/-}$ and *Stim1*$^{-/-}$; *Stim2*$^{-/-}$ MEFs increased Ca^{2+} entry rates by fivefold and eightfold, respectively, to values near to 70% of wild-type levels (Fig. 3A,C). The small levels of Ca^{2+} entry mediated by junctate alone, in *Stim1*$^{-/-}$; *Stim2*$^{-/-}$ MEFs, was abolished in the presence of the non-specific Ca^{2+} channel inhibitor lanthanum chloride (La^{3+}), similar to the STIM1-mediated entry, indicating that the source of the signal was extracellular (Fig. 3A,C). In addition, no significant change in intracellular Ca^{2+} was detected during Ca^{2+} removal and add-back in the absence of thapsigargin (Fig. 3B), indicating that the junctate-mediated entry was dependent on the emptying of ER Ca^{2+} stores. Taken together, these data indicate that junctate can have a small impact on global SOCE that is only revealed when both STIM proteins are absent.

Junctate boosts phagocytosis independently of STIM proteins

We next tested whether junctate expression impacts the ability of cells to phagocytose, using a high target:cell ratio (10:1) to increase the reliance of the phagocytic process on Ca^{2+} signals (Nunes et al., 2012). To synchronize the time of exposure to targets, RBCs were centrifuged onto cells that had been seeded onto coverslips, and cells were allowed to phagocytose for 30 min before fixation. This single timepoint snapshot provides an estimate of the phagocytic rate as cells reached their maximum phagocytic capacity, ∼2 h after target centrifugation at this target:cell ratio. Coverslips were immunostained to reveal c-Myc-tagged Fc receptors to facilitate phagosome identification, and imaged by using confocal microscopy. Quantification of confocal z-stacks through visual inspection revealed that the average number of phagocytosed particles per cell (the phagocytic index) during this 30-min time interval doubled in cells that expressed junctate compared to cells that expressed GFP–KDEL [wild type, 2.05±0.14 (GFP–KDEL)

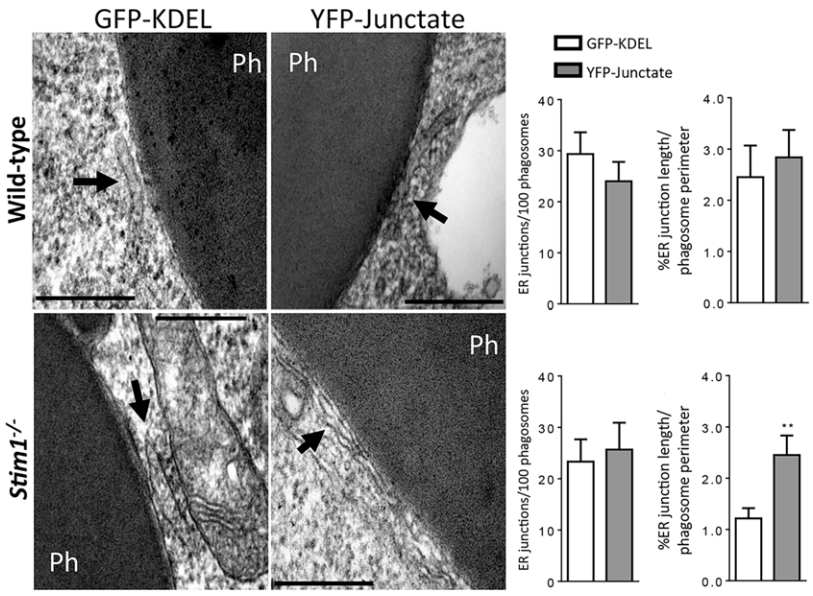

Fig. 2. Junctate expression increases the length of ER–phagosome membrane contact sites. Electron micrographs illustrating ER cisternae (arrows) juxtaposed to phagosomes (Ph) in wild-type (top panels) and *Stim1*$^{-/-}$ (bottom panels) MEFs. Quantitative analysis shows that the length of ER cisternae is significantly longer in cells overexpressing junctate (middle panels) in *Stim1*$^{-/-}$ MEFs (bottom right) but not in wild-type MEFs (top right). Qualitative differences of ER cisternae thickness can also be appreciated in *Stim1*$^{-/-}$ cells overexpressing junctate (arrows). Scale bars: 200 nm. Data are means±s.e.m. of three independent experiments comprising the following number of phagosomes, contacts. Wild type: KDEL, 101, 28; junctate, 87, 20. *Stim1*$^{-/-}$: KDEL, 110, 24; junctate, 101, 24. **P<0.01.

Journal of Cell Science (2015) 128, 4074-4082 doi:10.1242/jcs.172510

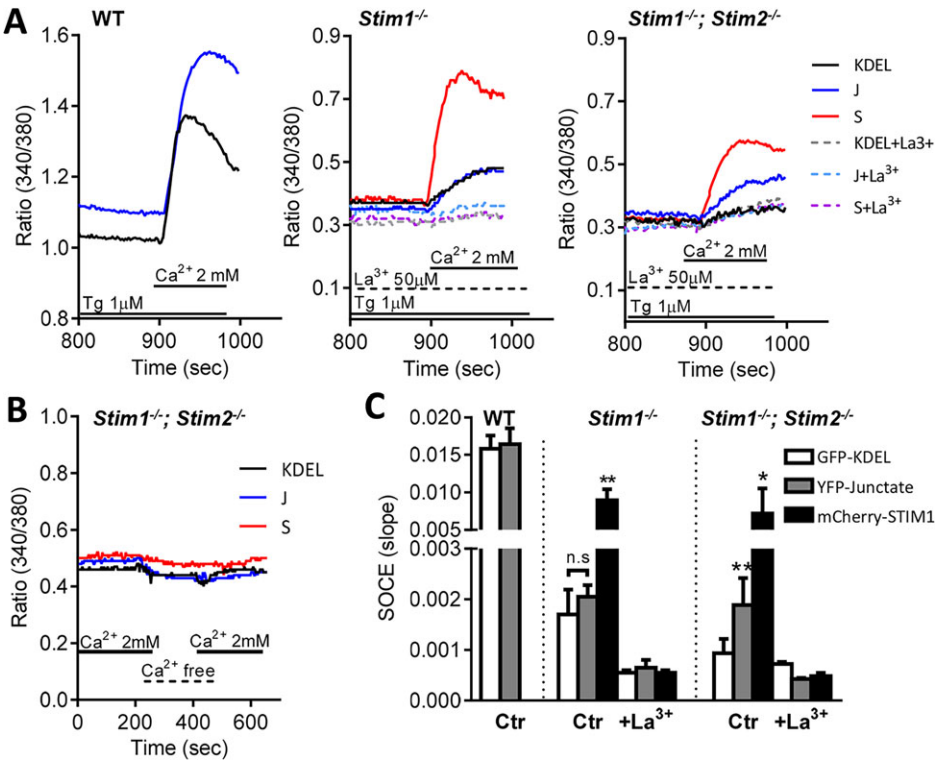

Fig. 3. Junctate increases SOCE, but only in the absence of both STIM proteins. (A) Representative changes in the ratio of Fura-2 fluorescence evoked by the addition of 2 mM Ca^{2+} to wild-type (WT, left panel), *Stim1*$^{-/-}$ (right panel) or *Stim1*$^{-/-}$*; Stim2*$^{-/-}$ MEFs that had been transfected with GFP–KDEL (black), YFP–junctate ('J', blue) and mCherry–STIM1 ('S', red) and treated with 1 µM thapsigargin (Tg) in Ca^{2+}-free medium to activate SOCE. Traces showing the inhibition of SOCE due to the use of 50 µM lanthanum chloride (La^{3+}) in *Stim1*$^{-/-}$ and *Stim1*$^{-/-}$*; Stim2*$^{-/-}$ MEFs transfected with GFP–KDEL (dotted grey), YFP–junctate (dotted light blue) and mCherry–STIM1 (dotted purple) are also shown (middle and right panels, respectively). (B) Representative changes in the ratio of Fura-2 fluorescence evoked by switching from 2 mM Ca^{2+} to Ca^{2+}-free medium, followed by 2 mM Ca^{2+} re-addition in the absence of thapsigargin in *Stim1*$^{-/-}$*; Stim2*$^{-/-}$ MEFs transfected with GFP–KDEL (black), YFP–junctate ('J', blue) and mCherry–STIM1 ('S', red) show that junctate expression does not lead to Ca^{2+} entry in the absence of store depletion. (C) Quantification of Ca^{2+} entry rates (slope) in *Stim1*$^{-/-}$, WT and *Stim1*$^{-/-}$*; Stim2*$^{-/-}$ cells shows that junctate does not increase SOCE unless both STIM1 proteins are absent and that this influx is abrogated by the non-specific SOCE channel inhibitor La^{3+}. Data are means±s.e.m. of three to eight independent experiments comprising 8–20 cells per experiment per condition. Ctr, control. **P*<0.05, ***P*<0.01.

and 3.76±0.47 (YFP–junctate) phagosomes per cell, mean±s.e.m. *n*=4 for each; *Stim1*$^{-/-}$, 1.58±0.21 and 3.03±0.35 phagosomes per cell, *n*=6 for each; *Stim1*$^{-/-}$*; Stim2*$^{-/-}$, 1.45±0.2 and 4.27±0.65 phagosomes per cell, *n*=6 for each; Fig. 4]. mCherry–STIM1 re-expression further boosted the phagocytic index (*Stim1*$^{-/-}$, to 4.15±0.79 phagosomes per cell, *n*=6; *Stim1*$^{-/-}$*; Stim2*$^{-/-}$, to 5.97±1.08 per cell, *n*=6; Fig. 4). These data suggest that junctate can increase the phagocytic capability of cells in the absence of STIM proteins despite having only a marginal effect on SOCE. The fact that *Stim1*$^{-/-}$*; Stim2*$^{-/-}$ cells showed similar or higher phagocytic rates and recruitment to phagosomes upon junctate overexpression indicates that junctate does not simply recruit STIM2 as an alternative mechanism to gate SOCE channels, and that, if anything, interaction with STIM2 could hinder junctate function, possibly by sequestering junctate elsewhere.

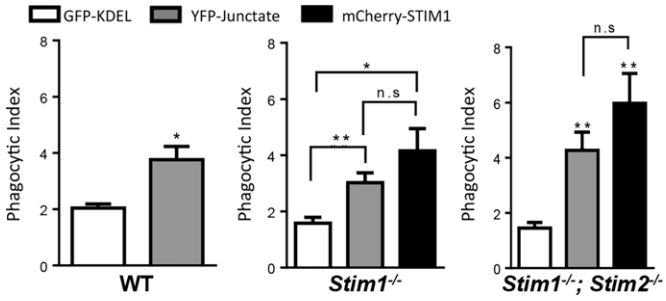

Fig. 4. Junctate increases the phagocytic capability of cells in the absence of STIM proteins. YFP–junctate but not GFP–KDEL overexpression boosts phagocytosis in wild-type (WT, left), *Stim1*$^{-/-}$ (middle) and *Stim1*$^{-/-}$*; Stim2*$^{-/-}$ (right) MEFs as efficiently as mCherry–STIM1. Data are means± s.e.m. of four to six independent experiments comprising the following total number of cells, phagosomes. Wild type: KDEL, 200, 402; junctate, 200, 746. *Stim1*$^{-/-}$: KDEL, 279, 458; junctate, 257, 769; STIM1, 310, 1407. *Stim1*$^{-/-}$*; Stim2*$^{-/-}$: KDEL, 190, 270; junctate, 152, 623; STIM1, 136, 724. n.s., not significant. **P*<0.05, ***P*<0.01.

Junctate increases the frequency of periphagosomal Ca^{2+} hotspots by promoting Ca^{2+} release from internal stores

Because STIM1 boosts phagocytosis by increasing the frequency and duration of local Ca^{2+} elevations around phagosomes, we assessed whether junctate also promotes periphagosomal Ca^{2+} elevations by using live confocal imaging and the Ca^{2+}-sensitive dye Fluo-8 (Fig. 5A). Ca^{2+} hotspots (arrows) were detected within a 750-nm perimeter (red region of interest, middle panel) in 6-s snapshots taken 25–30 min after the addition of phagocytic targets. Changes in hotspot occurrence in these snapshots might reflect either an increased frequency or duration of these events, both of which would reflect increased signaling. Although we did not observe changes in the temporal dynamics of hotspots (see Movie 1), approximately 39% of phagosomes in *Stim1*$^{-/-}$ cells that expressed red fluorescent protein (RFP)–KDEL as a control ER protein displayed periphagosomal Ca^{2+} hotspots, and this

Journal of Cell Science (2015) 128, 4074-4082 doi:10.1242/jcs.172510

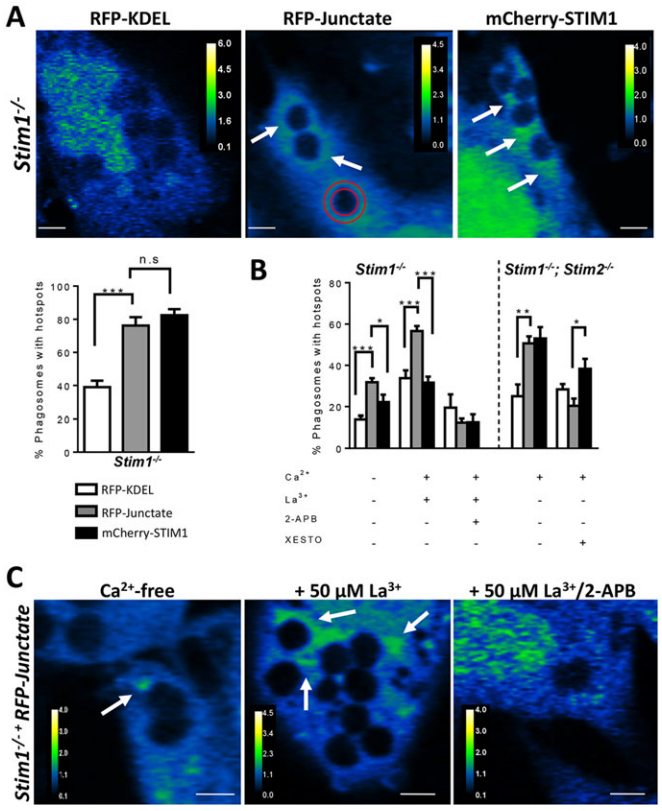

Fig. 5. Junctate boosts InsP3R-dependent Ca^{2+} release near phagosomes independently of STIM1. (A) Pseudo-colored (F/F_{0ave}) images of periphagosomal Ca^{2+} hotspots (arrows) in *Stim1*$^{-/-}$ MEFs overexpressing RFP–KDEL (left panel), RFP–junctate (middle panel) or mCherry–STIM1 (right panel) and loaded with 4 µM Fluo-8-AM in Ca^{2+}-containing medium. RFP–junctate and mCherry–STIM1 both doubled the occurrence of periphagosomal Ca^{2+} hotspots (bottom left panel). (B) Quantification of Ca^{2+}-hotspot frequencies revealed that RFP–junctate generated significantly more hotspots than mCherry–STIM1 in *Stim1*$^{-/-}$ MEFs when Ca^{2+} entry was prevented by Ca^{2+} removal or by the SOCE inhibitor La^{3+} (50 µM) but not when Ca^{2+} release was inhibited by the combination of La^{3+} and the InsP3R inhibitor 2-APB (50 µM). RFP–junctate is also able to generate significantly more hotspots than RFP–KDEL in *Stim1*$^{-/-}$*; Stim2*$^{-/-}$ MEFs, an effect prevented by xestospongin-C (20 µM). (C) Pseudo-colored (F/F_{0ave}) images of periphagosomal Ca^{2+} hotspots (arrows) in *Stim1*$^{-/-}$ MEFs loaded with 4 µM Fluo-8-AM, overexpressing RFP-junctate in Ca^{2+}-free medium (left panel), or in medium containing La^{3+} (50 µM, middle panel) or La^{3+}+2-APB (both at 50 µM, right panel). Colored bars, color-coded Fluo-8 fluorescence divided by the initial average cytosolic fluorescence (F/F_{0ave}). Scale bars: 3 µm. Data are means±s.e.m. of three to six independent experiments comprising the following number of cells, phagosomes. *Stim1*$^{-/-}$: KDEL, 54, 524; junctate, 78, 589; STIM1, 67, 648. *Stim1*$^{-/-}$+Ca^{2+}-free medium: KDEL, 121, 417; junctate, 212, 840; STIM1, 130, 517. *Stim1*$^{-/-}$ La^{3+}: KDEL, 127, 272; junctate, 151, 487; STIM1, 99, 312. *Stim1*$^{-/-}$ La^{3+}+2-APB: KDEL, 93, 88; junctate, 91, 140; STIM1, 61, 89. *Stim1*$^{-/-}$*; Stim2*$^{-/-}$ Ca^{2+}-containing medium: KDEL, 50, 120; junctate, 37, 126; STIM1, 28, 113. *Stim1*$^{-/-}$*; Stim2*$^{-/-}$+xestospongin-C: KDEL, 35, 108; junctate, 37, 72; STIM1, 32, 104. n.s., not significant. **P*<0.05, ***P*<0.01, ****P*<0.001.

percentage increased to 76% and 82% upon expression of RFP–junctate and mCherry–STIM1, respectively (*n*=5 for all conditions; Fig. 5A, bottom panel). Thus, junctate is as efficient as STIM1 in promoting periphagosomal Ca^{2+} elevations. Interestingly, although the hotspots promoted by junctate covered a similar fraction of the phagosomal surface as the STIM1-generated hotspots (28% vs 27%, *n*=47 and 64 phagosomes, respectively), they extended more frequently beyond the 750-nm wide periphagosomal space (84±5.0% vs 59±4.5%, *n*=3), prompting us to further explore the source of the Ca^{2+} signal. The intracellular Ca^{2+} hotspots that form around phagosomes can reflect either Ca^{2+} release from the ER or Ca^{2+} release from phagosomes, which initially contain a high concentration of Ca^{2+} that is derived from the extracellular space. To distinguish between these two sources of Ca^{2+}, we repeated the experiment either in Ca^{2+}-free medium or in the presence of SOCE channel inhibitor La^{3+}, which abolished global SOCE in *Stim1*$^{-/-}$ and *Stim1*$^{-/-}$*; Stim2*$^{-/-}$ cells (Fig. 3A,C). This generic Ca^{2+}-channel blocker is internalized into the lumen of forming phagosomes and minimizes the contribution of Ca^{2+} flowing across both plasma-membrane and phagosomal channels, allowing us to isolate the Ca^{2+} signals originating from internal stores. Ca^{2+} removal from the external medium decreased the percentage of phagosomes that were associated with local Ca^{2+} elevations to 14% and 22% in RFP–KDEL and mCherry–STIM1 cells, respectively, but to only 32% in cells that expressed RFP–junctate, which exhibited significantly more periphagosomal Ca^{2+} microdomains than cells that expressed the other two proteins (Fig. 5B,C). This difference was further increased in the presence of La^{3+}, which had only a mild effect on the activity recorded in RFP–junctate-expressing cells but decreased the activity of mCherry–STIM1-expressing cells to control levels (55% for RFP–junctate versus 34% and 36% for RFP–KDEL and mCherry–STIM1, respectively; Fig. 5B,C).

To confirm that junctate regulates periphagosomal Ca^{2+} hotspots by recruiting functional Ca^{2+} stores, periphagosomal Ca^{2+} was measured in the presence of the InsP3R inhibitor 2-APB. Because 2-APB also blocks Orai channels, La^{3+} was simultaneously applied to eliminate the contribution of any SOCE channel, including Orai-family proteins. This treatment decreased the frequency of periphagosomal Ca^{2+} hotspots to control levels in both RFP–junctate- and mCherry–STIM1-expressing cells (12% for RFP–junctate vs 19% for RFP–KDEL and 13% for mCherry–STIM1; Fig. 5B,C). Finally, to control for the contribution of residual STIM2-mediated channel gating, periphagosomal Ca^{2+} hotspots were also quantified in *Stim1*$^{-/-}$*; Stim2*$^{-/-}$ MEFs. Similar to *Stim1*$^{-/-}$ cells, YFP–junctate and mCherry–STIM1 expression increased hotspot frequency by twofold, to 51% and 53% respectively, compared to 25% for RFP–KDEL (Fig. 5B). Xestospongin-C, a more specific InsP3R blocker that suppressed ATP-induced Ca^{2+} signals in *Stim1*$^{-/-}$*; Stim2*$^{-/-}$ MEFs (Fig. S1), had no effect on hotspot frequency in cells that expressed RFP–KDEL but did abrogate the increase in periphagosomal Ca^{2+} hotspots evoked by junctate expression and decreased the frequency of the STIM1-induced hotspots to 38% (Fig. 5B). The residual Ca^{2+} hotspots persisting in the presence of inhibitors might reflect incomplete inhibition of Ca^{2+} influx and release channels, or release from InsP3R-independent Ca^{2+} stores. Taken together, these data confirm that STIM1-mediated hotspots are generated by both phagosomal and ER-store release components, as previously suggested, and show that the store release component is InsP3R-dependent. Moreover, these results indicate that junctate promotes periphagosomal Ca^{2+} elevations primarily by recruiting functional Ca^{2+} stores to phagosomes rather than by interacting with Ca^{2+}-permeable channels that are present in the phagosome membrane.

Junctate promotes phagosomal actin shedding

Periphagosomal Ca^{2+} hotspots have been previously shown to promote shedding of the actin coat that forms during phagosomal ingestion, which is considered to be an important stage during early phagosome maturation (Nunes and Demaurex, 2010; Nunes et al.,

Journal of Cell Science (2015) 128, 4074-4082 doi:10.1242/jcs.172510

2012). Reduced actin shedding might limit global phagocytic rates by hindering phagosome–lysosome fusion as well as fission events that allow recycling of Fc receptors back to the cell surface. The availability of actin, and particularly rapid actin dynamics, could be additionally important for higher speeds of subsequent actin-driven membrane remodeling as the cell internalizes new targets. We thus further investigated whether junctate, like STIM1, influences periphagosomal actin structures. Both in *Stim1*$^{-/-}$ and *Stim1*$^{-/-}$; *Stim2*$^{-/-}$ MEFs, the overexpression of RFP–junctate and mCherry–STIM1 decreased periphagosomal filamentous F-actin rings compared to that in RFP–KDEL controls (Fig. 6). These data indicate that junctate regulates phagocytic ingestion rates by promoting periphagosomal actin shedding.

DISCUSSION

In this study, we show that junctate is an important signaling protein that can determine the efficiency of the phagocytic process. We provide morphological evidence that junctate is recruited to phagosomes and increases the length of juxtaposed ER structures, and functional evidence that junctate significantly increases the efficiency of phagocytosis independently of STIM1. We could link the pro-phagocytic effects of junctate to an increased frequency of periphagosomal Ca^{2+} elevations occurring near phagosomes, as well as to increased actin shedding during early phagosome maturation, and show that the junctate-associated Ca^{2+} hotspots or microdomains are much less affected by Ca^{2+} removal and by the SOCE channel inhibitor La^{3+} than STIM1-associated Ca^{2+} microdomains. We further show that the junctate-associated Ca^{2+} microdomains are almost abrogated by the InsP3R inhibitor 2-APB in the presence of La^{3+}, as well as by the more specific InsP3R inhibitor xestospongin-C alone, indicating that they essentially reflect Ca^{2+} release from inositol-trisphosphate-sensitive stores. This suggests that, unlike STIM1, junctate does not promote the opening of phagosomal Ca^{2+} channels but instead recruits InsP3R-containing ER Ca^{2+} stores near phagosomes. Junctate is more efficient than STIM1 in recruiting functional ER Ca^{2+} stores, whereas STIM1 is more efficient in gating phagosomal Ca^{2+} channels, allowing the two proteins to cooperate to promote the generation of local Ca^{2+} elevations that boost phagocytosis.

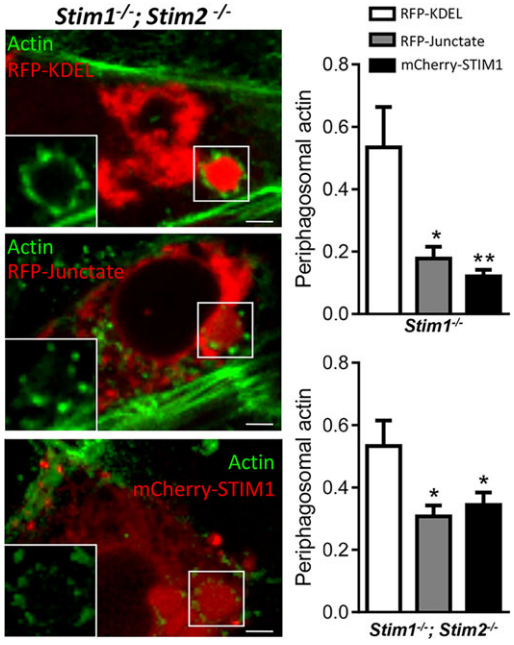

Fig. 6. Junctate overexpression promotes actin shedding. Three-dimensional projections of confocal *z*-stacks show that the appearance of F-actin rings (green, left panels) was decreased around phagosomes when RFP–junctate and mCherry–STIM1 (red) were overexpressed in both *Stim1*$^{-/-}$ (top right panel) and *Stim1*$^{-/-}$; *Stim2*$^{-/-}$ (bottom right panel and images) MEFs. The bar graphs represent the average phalloidin–FITC intensity in a 1-µm ring surrounding the midsection of a given phagosome, normalized to the total phalloidin staining of the cell. Scale bars: 3 µm. Data are means±s.e.m. of three independent experiments, comprising the following total number of phagosomes. *Stim1*$^{-/-}$: KDEL, 56; junctate, 96; STIM1, 93. *Stim1*$^{-/-}$; *Stim2*$^{-/-}$: KDEL, 35; junctate, 56; STIM1, 49. *P<0.05, **P<0.01.

Junctate has previously been shown to play an important role in Ca^{2+} homeostasis and to interact with several components of the Ca^{2+} 'toolkit'. Initial studies reported that junctate interacts through its cytosolic N-terminal domain with the InsP3R and TRPC channels, and that junctate overexpression increases agonist-induced Ca^{2+} elevations, whereas silencing has the opposite effect (Treves et al., 2004). Those authors have subsequently shown that junctate stabilizes ER–plasma-membrane junctions and promotes agonist-activated Ca^{2+} entry across TRPC3 channels (Treves et al., 2010). Junctate also interacts with SERCA2a in cardiomyocytes (Kwon and Kim, 2009), and with TRPC2 and TRPC5 channels in rodent sperm (Stamboulian et al., 2005). More recently, junctate has been shown to interact through its luminal domain with STIM1 and to provide an alternative mechanism for STIM1 recruitment to Ca^{2+} entry sites at the plasma membrane (Srikanth et al., 2012). In this study, junctate overexpression in primary T cells caused a marginal increase in SOCE, whereas a junctate EF-hand mutant promoted the accumulation of STIM1 in ER–plasma-membrane clusters and caused a marked increase in SOCE. These data indicate that junctate acts as an ER sensor that facilitates STIM1 clustering at ER–plasma-membrane junctions, but they do not exclude the possibility that junctate acts as a ligand for membrane channels on its own in response to store depletion. We observed that when SOCE is maximally activated, junctate overexpression does not further increase global Ca^{2+} entry rates in wild-type MEFs, nor does it rescue the residual SOCE of *Stim1*$^{-/-}$ cells. By contrast, it can induce a small but significant SOCE in the complete absence of STIM proteins. This surprising result suggests that junctate can gate SOCE channels independently of STIM proteins. This observation not only lends further insight into the function of junctate, but adds an additional layer to the complex regulation of store-operated Ca^{2+} entry by identifying an additional ER Ca^{2+} sensor, beyond the three known STIM protein isoforms STIM1, STIM1L and STIM2. Because junctate is known to bind to TRPC-family channels, and because the non-specific Ca^{2+} channel blocker La^{3+} abolished junctate-mediated influx, TRPCs are the prime candidates for serving as junctate partners, and further study will be required to identify the exact partner channels as well as whether other physiological functions are linked to this additional influx mechanism. Junctate–TRPC interactions could explain the fact that, in RFP–junctate-expressing cells, La^{3+} slightly decreased the fraction of phagosomes that had Ca^{2+} microdomains (from 76% to 57%; Fig. 5A,B) in *Stim1*$^{-/-}$ cells. However, this could also reflect reduced Ca^{2+} release from stores, because La^{3+} could prevent store refilling by inhibiting plasma membrane Ca^{2+} channels during the phagocytic process. In any case, La^{3+} was much more effective in STIM1-expressing cells, impacting the majority of the Ca^{2+} -signaling around those phagosomes (from 82% to 36%; Fig. 5B). Thus, the STIM1–Orai interactions that take place at the ER–phagosome interface are much more efficient than the putative junctate–TRPC interactions in promoting the opening of phagosomal Ca^{2+} channels.

Journal of Cell Science (2015) 128, 4074-4082 doi:10.1242/jcs.172510

Our *Stim1*$^{-/-}$ phagocytic cells provided a useful model system to highlight the similarities and differences between STIM1 and junctate. Both STIM1 and junctate were recruited to phagosomes in *Stim1*$^{-/-}$ cells, demonstrating that junctate is recruited independently of STIM1, and the two proteins populated the same periphagosomal structures when co-expressed. Junctate is localized at ER–plasma-membrane contact sites before store depletion through its N-terminal domain (Srikanth et al., 2012; Treves et al., 2010), but whether junctate is 'pre-addressed' to contact sites through this targeting motif or responds to smaller or localized store depletion compared to STIM1 is unclear. The STIM1 luminal domain has been estimated to have a Ca^{2+}-binding K_d of 200–600 µM *in vitro* (Stathopulos et al., 2006), and 169–210 µM by using fluorescence and patch-clamp recordings (Brandman et al., 2007; Luik et al., 2008). The K_d of junctate has been estimated to be around 217±20 µM by using fluorescence imaging (Treves et al., 2000).We cannot establish whether junctate is recruited to phagosomes independently of store depletion because the Ca^{2+} concentration within the ER lumen decreases as soon as phagocytic receptors are engaged, which could initiate the recruitment of junctate to its target membranes. Whether an additional signal triggers the accumulation of junctate at the ER–phagosome interface or alternatively, whether phagosomes form preferentially around pre-existing junctate-containing ER–plasma-membrane contact sites therefore remains to be determined.

Our electron microscopy data also establish that junctate is an ER-shaping protein that can elongate ER cisternae that are apposed to phagosomes, causing a doubling in their length (from 115 to 231 nm; Fig. 2). This effect was most apparent in the absence of STIM1 because junctate expression in wild-type fibroblasts only marginally increased the already larger size of the recruited ER structures (from 231 to 268 nm; Fig. 2). Previous studies have reported that junctate expression extends ER–plasma-membrane contacts by up to 55% (from 218 to 339 nm) in HEK-293 cells (Treves et al., 2004). We confirm here that junctate is indeed able to elongate ER structures and further establish that this effect is independent of STIM1. In wild-type MEFs, juxtaposed ER might already be near to maximal length owing to high levels of endogenous STIM1, but differences in junctate localization and overexpression efficiency might also explain the lack of lengthening effect in these cells. Compared to STIM1, junctate was less efficient in remodeling the ER because its expression did not promote the appearance of new ER structures that were apposed to phagosomes, only their extension. It should be noted however that we only quantified ER structures that were located less than 30 nm from the phagosomal membrane. Junctate might, in fact, be more efficient than STIM1 in recruiting ER structures at some distance from the phagosomes, as suggested by the fluorescence pattern of periphagosomal YFP–junctate. The physiological role of the ER extension mediated by STIM1 and junctate is unclear. The enlargement of ER–plasma-membrane junctions that is mediated by different STIM1 isoforms does not correlate with an increase in SOCE or in the efficiency of ER Ca^{2+} refilling (Saüc et al., 2015), suggesting that elongation is not related to the Ca^{2+}-signaling function of STIM1 molecules. The enlargement of juxtaposed ER structures might provide more stable signaling platforms for interactions of ER proteins with their ligands at the plasma or phagosomal membrane, or for lipid exchange between the two juxtaposed membranes (Toulmay and Prinz, 2011). At the ER–phagosome interface, the extension might promote the cross-presentation of antigens processed within the phagosomes, which relies on the communication between phagosomes and the ER-resident antigen loading machinery in a manner that is still poorly understood (Blum et al., 2013).

To conclude, our data further the understanding of junctate function as an important component of ER membrane contact sites, platforms that allow cells to precisely localize Ca^{2+} signals within cells. We showed that junctate complements STIM1 function, independently increasing contact lengths and Ca^{2+} release from stores near to phagosomes, thereby increasing phagocytic efficiency. Although our work is focused within the context of an important process of immune cell function – that of phagocytosis – in a more general sense, our data illustrate that, when global Ca^{2+} signals are abrogated, increasing localized Ca^{2+} signals through Ca^{2+} release from stores can provide an effective compensatory mechanism when SOCE is naturally, pathologically or therapeutically inhibited. This might be a concept with repercussions beyond the field of phagocytosis because Ca^{2+} signaling is important for many cell types and for a variety of cellular functions, including cell growth, apoptosis, secretion, contraction and motility. Furthermore, because SOCE channels have been proposed as drug targets in therapeutic avenues for diseases including cancer and autoimmune disorders, a better understanding of complementary or compensatory mechanisms of Ca^{2+} signaling will undoubtedly lead to more intelligent therapeutic designs.

MATERIALS AND METHODS

Reagents

Stim1$^{-/-}$ MEFs, generated through targeted gene disruption (Prins et al., 2011), and wild-type MEF control cells were a kind gift from Dr Marek Michalak (University of Alberta, Canada). YFP-tagged junctate was a kind gift from Dr Susan Treves (University of Basel, Switzerland). Dulbecco's modified Eagle's medium (DMEM; high glucose, catalog number 31966), heat-inactivated fetal calf serum (FCS), penicillin–streptomycin mixture (pen–strep, catalog number 15140), Fura-2-AM, BAPTA-AM, Lipofectamine 2000 transfection reagent, goat-anti-mouse conjugated to Alexa-Fluor-647 (1:1000) and SlowFade mounting medium were obtained from Life Technologies. Quest Fluo-8-AM was purchased from AAT Bioquest (Sunnyvale, CA). Mouse anti-Myc-tag antibody (9B11, 1:100) was purchased from Cell Signaling. Gluteraldehyde-stabilized sheep red blood cells (sRBCs), rabbit anti-sRBCs (1:200) and all other chemicals were obtained from Sigma-Aldrich. To reduce autofluorescence, gluteraldehyde-stabilized sRBCs were treated with bubbling 0.6% $NaBH_4$ in PBS with agitation for 1 h, washed three times in PBS and stored frozen.

Cell culture and transfection

MEFs were grown in DMEM containing 10% FCS and 0.5% pen–strep at 37°C under 5% CO_2 and were passaged twice a week. Cells were used between passages 5 and 50. Transfections were performed with Lipofectamine 2000 with cells at 50–60% confluence in high glucose (4.5 g/l) DMEM. Transfected cells were allowed to recover for 24 h before manipulation.

Phagocytosis and ER protein recruitment to phagosomes

Opsonization was performed the same day as phagocytosis experiments. RBCs were opsonized by rabbit-anti-sheep RBCs at 37°C for 1 h and washed three times in PBS. Targets were added directly to cells that had been seeded on 12-mm coverslips in 24-well plates at 10:1 target:cell ratio in serum-containing medium. Plates containing coverslips were centrifuged at 600 ***g*** for 1 min. Cells were then incubated at 37 °C under 5% CO_2 for 10 min in the case of ER recruitment experiments and 30 min for phagocytosis experiments, before fixation and immunolabeling.

Immunolabeling

Cells were fixed in 4% paraformaldehyde in PBS. Fixed cells were permeabilized and blocked in 0.3% Triton X-100 with 1% BSA in PBS, and

incubated overnight at 4°C in primary antibody (mouse antibody against Myc tag, 1:100). The following day, cells were incubated for 1 h in secondary antibody (goat anti-mouse, conjugated to Alexa-Fluor-647, 1:1000) and then washed three times with PBS. Coverslips were mounted in SlowFade mounting medium containing 1 µg/µl Hoechst 33342.

Electron microscopy

Cells were fixed for 1 h in 2% glutaraldehyde with 0.1 M $NaPO_4$, pH 7.4, and scraped, and the pellets were washed once in 0.1 M sodium phosphate buffer, pH 7.4. En bloc staining with uranyl acetate, postfixation with osmium tetroxide, dehydration in ethanol, embedding in Epon and sectioning were performed by the Pole Facultaire de Microscopie Electronique core facility at the University of Geneva. Two grids per independent sample containing 8–10 50-nm sections were observed using a Tecnai transmission electron microscope (FEI, Eindhoven, The Netherlands). Of these, all phagosomes that could be identified in two to three randomly selected intact sections were examined. Quantification was performed using XT Pro software (Soft Imaging System GmbH, Germany).

Imaging

All fixed-cell imaging was performed using a confocal laser scanning microscope (LSM 700, Carl Zeiss AG) equipped with a 60× objective. Fura-2 imaging was performed using a wide-field fluorescence microscope equipped with a 40× objective, polychromator illumination, 430DCLP dichroic and 510WB40 emission filter (Visitron Systems, GmbH). Here, the fluorescence of YFP and GFP, or of RFP tags in transfected cells was simultaneously examined, and cells expressing very high levels of transfected proteins or showing signs of pre-activation or toxicity were eliminated from the analysis. Fluo-8 imaging was performed using a Nikon A1R inverted confocal microscope system equipped with 60× objective and a resonant scanner, and maintained at 37°C by a microscope temperature control system (Life Imaging Services, Basel, Switzerland). Fluo-8 fluorescence was imaged using the 488-nm laser line, whereas the autofluorescence of RBCs was imaged using the far-red 633-nm laser. Experiments were performed in physiological buffer – 140 mM NaCl, 5 mM KCl, 1 mM $MgCl_2$, 2 mM $CaCl_2$, 20 mM Hepes, 10 mM glucose, adjusted to pH 7.4, with NaOH. Ca^{2+}-free medium contained 1 mM EGTA instead of 2 mM $CaCl_2$. Fura-2-AM (2 µM) was loaded in physiological buffer with 0.02% pluronic and visualized using 340/380-nm alternate excitation and 510±40-nm emission. Frames were acquired every 2 s. Fluo8-AM (4 µM) was loaded in physiological buffer with 250 µM sulfinpyrazone at 37°C for 30 min. This was followed by incubation for 20 min at room temperature and subsequent addition of BAPTA-AM (5 µM) for another 10 min. For quantification of phagocytosis, ER protein recruitment and periphagosomal Ca^{2+} hotspots, the same protocol that has been previously described for STIM1 was used (Nunes et al., 2012), except for Ca^{2+}-free experiments, where instead of using 3 mM EDTA to chelate extracellular 2 mM Ca^{2+}, the experiment was performed in Ca^{2+}-free medium. Briefly, for phagocytosis and ER protein recruitment studies, at least three confocal *z*-stacks of equal dimensions (~15 µm thickness at 0.5 µm steps) per coverslip were imaged, and at least n=3 independent experiments were quantified for each condition. RBCs completely enclosed by cellular borders were defined as phagosomes. For RBCs found near the cell periphery, in the case of incomplete enclosure, only RBCs with ≥75% of their surface surrounded by Fc receptor immunoreactivity were counted as phagosomes. ER proteins were considered to be recruited to the vicinity of phagosomes when bright fluorescent clusters (puncta) could be detected by visual inspection in the space within 3 pixels (~750 nm) of phagosomes. Ca^{2+} hotspots were defined as regions of an area ≥500 nm^2 (4 pixels) within a distance of ~750 nm (3 pixels) from the phagosomal border displaying fluorescence at least 2 s.d. higher than the average cytoplasmic Fluo-8 intensity. At least five snapshots per coverslip and at least n=3 independent coverslips were quantified for each condition.

Statistics

All statistical analyses were performed using Prism software (GraphPad). Significance between two sets of experiments was determined using an unpaired Student's *t*-test.

Acknowledgements

We are grateful to Mr Cyril Castelbou for excellent technical assistance, to the bioimaging core facility (Geneva Medical Center) and to Dr Maud Frieden and Dr Claes Wollheim for advice and for critical reading of the manuscript.

Competing interests

The authors declare no competing or financial interests.

Author contributions

P.N. and N.D. designed research; D.G. and P.N. performed research and analyzed data; D.G., P.N. and N.D. wrote the paper. N.D. and P.N. contributed equally as senior authors to this manuscript.

Funding

This work was funded by the Swiss National Foundation [grant number 31003A-149566 (to N.D.)]; and a Young Investigator Subsidy from The Sir Jules Thorn Overseas Charitable Trust (to P.N.).

Supplementary information

Supplementary information available online at
http://jcs.biologists.org/lookup/suppl/doi:10.1242/jcs.172510/-/DC1

References

Aderem, A. and Underhill, D. M. (1999). Mechanisms of phagocytosis in macrophages. *Annu. Rev. Immunol.* **17**, 593-623.

Bengtsson, T., Jaconi, M. E., Gustafson, M., Magnusson, K. E., Theler, J. M., Lew, D. P. and Stendahl, O. (1993). Actin dynamics in human neutrophils during adhesion and phagocytosis is controlled by changes in intracellular free calcium. *Eur. J. Cell Biol.* **62**, 49-58.

Blum, J. S., Wearsch, P. A. and Cresswell, P. (2013). Pathways of antigen processing. *Annu. Rev. Immunol.* **31**, 443-473.

Brandman, O., Liou, J., Park, W. S. and Meyer, T. (2007). STIM2 is a feedback regulator that stabilizes basal cytosolic and endoplasmic reticulum Ca2+ levels. *Cell* **131**, 1327-1339.

Dewitt, S., Laffafian, I. and Hallett, M. B. (2003). Phagosomal oxidative activity during beta2 integrin (CR3)-mediated phagocytosis by neutrophils is triggered by a non-restricted Ca2+ signal: Ca2+ controls time not space. *J. Cell Sci.* **116**, 2857-2865.

Dinchuk, J. E., Henderson, N. L., Burn, T. C., Huber, R., Ho, S. P., Link, J., O'Neil, K. T., Focht, R. J., Scully, M. S., Hollis, J. M. et al. (2000). Aspartyl beta -hydroxylase (Asph) and an evolutionarily conserved isoform of Asph missing the catalytic domain share exons with junctin. *J. Biol. Chem.* **275**, 39543-39554.

Feske, S., Gwack, Y., Prakriya, M., Srikanth, S., Puppel, S.-H., Tanasa, B., Hogan, P. G., Lewis, R. S., Daly, M. and Rao, A. (2006). A mutation in Orai1 causes immune deficiency by abrogating CRAC channel function. *Nature* **441**, 179-185.

Hogan, P. G., Lewis, R. S. and Rao, A. (2010). Molecular basis of calcium signaling in lymphocytes: STIM and ORAI. *Annu. Rev. Immunol.* **28**, 491-533.

Hong, C.-S., Kwak, Y.-G., Ji, J.-H., Chae, S.-W. and Han Kim, D. (2001). Molecular cloning and characterization of mouse cardiac junctate isoforms. *Biochem. Biophys. Res. Commun.* **289**, 882-887.

Hong, C.-S., Kwon, S.-J., Cho, M.-C., Kwak, Y.-G., Ha, K.-C., Hong, B., Li, H., Chae, S.-W., Chai, O.-H., Song, C. H. et al. (2008). Overexpression of junctate induces cardiac hypertrophy and arrhythmia via altered calcium handling. *J. Mol. Cell. Cardiol.* **44**, 672-682.

Huang, G. N., Zeng, W., Kim, J. Y., Yuan, J. P., Han, L., Muallem, S. and Worley, P. F. (2006). STIM1 carboxyl-terminus activates native SOC, Icrac and TRPC1 channels. *Nat. Cell Biol.* **8**, 1003-1010.

Jaconi, M. E., Lew, D. P., Carpentier, J. L., Magnusson, K. E., Sjögren, M. and Stendahl, O. (1990). Cytosolic free calcium elevation mediates the phagosome-lysosome fusion during phagocytosis in human neutrophils. *J. Cell Biol.* **110**, 1555-1564.

Kwon, S.-J. and Kim, D. H. (2009). Characterization of junctate–SERCA2a interaction in murine cardiomyocyte. *Biochem. Biophys. Res. Commun.* **390**, 1389-1394.

Liou, J., Kim, M. L., Do Heo, W., Jones, J. T., Myers, J. W., Ferrell, J. E., Jr. and Meyer, T. (2005). STIM is a Ca2+ sensor essential for Ca2+-store-depletion-triggered Ca2+ influx. *Curr. Biol.* **15**, 1235-1241.

Luik, R. M., Wu, M. M., Buchanan, J. and Lewis, R. S. (2006). The elementary unit of store-operated Ca2+ entry: local activation of CRAC channels by STIM1 at ER-plasma membrane junctions. *J. Cell Biol.* **174**, 815-825.

Luik, R. M., Wang, B., Prakriya, M., Wu, M. M. and Lewis, R. S. (2008). Oligomerization of STIM1 couples ER calcium depletion to CRAC channel activation. *Nature* **454**, 538-542.

Lur, G., Haynes, L. P., Prior, I. A., Gerasimenko, O. V., Feske, S., Petersen, O. H., Burgoyne, R. D. and Tepikin, A. V. (2009). Ribosome-free terminals of rough ER

allow formation of STIM1 puncta and segregation of STIM1 from IP3 receptors. *Curr. Biol.* **19**, 1648-1653.

Muik, M., Fahrner, M., Derler, I., Schindl, R., Bergsmann, J., Frischauf, I., Groschner, K. and Romanin, C. (2009). A cytosolic homomerization and a modulatory domain within STIM1 C terminus determine coupling to ORAI1 channels. *J. Biol. Chem.* **284**, 8421-8426.

Nunes, P. and Demaurex, N. (2010). The role of calcium signaling in phagocytosis. *J. Leukoc. Biol.* **88**, 57-68.

Nunes, P., Cornut, D., Bochet, V., Hasler, U., Oh-Hora, M., Waldburger, J.-M. and Demaurex, N. (2012). STIM1 juxtaposes ER to phagosomes, generating Ca2+ hotspots that boost phagocytosis. *Curr. Biol.* **22**, 1990-1997.

Orci, L., Ravazzola, M., Le Coadic, M., Shen, W.-w., Demaurex, N. and Cosson, P. (2009). STIM1-induced precortical and cortical subdomains of the endoplasmic reticulum. *Proc. Natl. Acad. Sci. USA* **106**, 19358-19362.

Park, C. Y., Hoover, P. J., Mullins, F. M., Bachhawat, P., Covington, E. D., Raunser, S., Walz, T., Garcia, K. C., Dolmetsch, R. E. and Lewis, R. S. (2009). STIM1 clusters and activates CRAC channels via direct binding of a cytosolic domain to Orai1. *Cell* **136**, 876-890.

Prins, D., Groenendyk, J., Touret, N. and Michalak, M. (2011). Modulation of STIM1 and capacitative Ca2+ entry by the endoplasmic reticulum luminal oxidoreductase ERp57. *EMBO Rep.* **12**, 1182-1188.

Roos, J., DiGregorio, P. J., Yeromin, A. V., Ohlsen, K., Lioudyno, M., Zhang, S., Safrina, O., Kozak, J. A., Wagner, S. L., Cahalan, M. D. et al. (2005). STIM1, an essential and conserved component of store-operated Ca2+ channel function. *J. Cell Biol.* **169**, 435-445.

Saüc, S., Bulla, M., Nunes, P., Orci, L., Marchetti, A., Antigny, F., Bernheim, L., Cosson, P., Frieden, M. and Demaurex, N. (2015). STIM1L traps and gates Orai1 channels without remodeling the cortical ER. *J. Cell Sci.* **128**, 1568-1579.

Srikanth, S., Jew, M., Kim, K.-D., Yee, M.-K., Abramson, J. and Gwack, Y. (2012). Junctate is a Ca2+-sensing structural component of Orai1 and stromal interaction molecule 1 (STIM1). *Proc. Natl. Acad. Sci. USA* **109**, 8682-8687.

Stamboulian, S., Moutin, M.-J., Treves, S., Pochon, N., Grunwald, D., Zorzato, F., De Waard, M., Ronjat, M. and Arnoult, C. (2005). Junctate, an inositol 1,4,5-triphosphate receptor associated protein, is present in rodent sperm and binds TRPC2 and TRPC5 but not TRPC1 channels. *Dev. Biol.* **286**, 326-337.

Stathopulos, P. B., Li, G.-Y., Plevin, M. J., Ames, J. B. and Ikura, M. (2006). Stored Ca2+ depletion-induced oligomerization of stromal interaction molecule 1 (STIM1) via the EF-SAM region: an initiation mechanism for capacitive Ca2+ entry. *J. Biol. Chem.* **281**, 35855-35862.

Toulmay, A. and Prinz, W. A. (2011). Lipid transfer and signaling at organelle contact sites: the tip of the iceberg. *Curr. Opin. Cell Biol.* **23**, 458-463.

Treves, S., Feriotto, G., Moccagatta, L., Gambari, R. and Zorzato, F. (2000). Molecular cloning, expression, functional characterization, chromosomal localization, and gene structure of junctate, a novel integral calcium binding protein of sarco(endo)plasmic reticulum membrane. *J. Biol. Chem.* **275**, 39555-39568.

Treves, S., Franzini-Armstrong, C., Moccagatta, L., Arnoult, C., Grasso, C., Schrum, A., Ducreux, S., Zhu, M. X., Mikoshiba, K., Girard, T. et al. (2004). Junctate is a key element in calcium entry induced by activation of InsP3 receptors and/or calcium store depletion. *J. Cell Biol.* **166**, 537-548.

Treves, S., Vukcevic, M., Griesser, J., Armstrong, C.-F., Zhu, M. X. and Zorzato, F. (2010). Agonist-activated Ca2+ influx occurs at stable plasma membrane and endoplasmic reticulum junctions. *J. Cell Sci.* **123**, 4170-4181.

Vig, M., Peinelt, C., Beck, A., Koomoa, D. L., Rabah, D., Koblan-Huberson, M., Kraft, S., Turner, H., Fleig, A., Penner, R. et al. (2006). CRACM1 is a plasma membrane protein essential for store-operated Ca2+ entry. *Science* **312**, 1220-1223.

Walsh, C. M., Chvanov, M., Haynes, L. P., Petersen, O. H., Tepikin, A. V. and Burgoyne, R. D. (2010). Role of phosphoinositides in STIM1 dynamics and store-operated calcium entry. *Biochem. J.* **425**, 159-168.

Wu, M. M., Buchanan, J., Luik, R. M. and Lewis, R. S. (2006). Ca2+ store depletion causes STIM1 to accumulate in ER regions closely associated with the plasma membrane. *J. Cell Biol.* **174**, 803-813.

Xu, P., Lu, J., Li, Z., Yu, X., Chen, L. and Xu, T. (2006). Aggregation of STIM1 underneath the plasma membrane induces clustering of Orai1. *Biochem. Biophys. Res. Commun.* **350**, 969-976.

Yuan, J. P., Zeng, W., Dorwart, M. R., Choi, Y.-J., Worley, P. F. and Muallem, S. (2009). SOAR and the polybasic STIM1 domains gate and regulate Orai channels. *Nat. Cell Biol.* **11**, 337-343.

Zhang, S. L., Yu, Y., Roos, J., Kozak, J. A., Deerinck, T. J., Ellisman, M. H., Stauderman, K. A. and Cahalan, M. D. (2005). STIM1 is a Ca2+ sensor that activates CRAC channels and migrates from the Ca2+ store to the plasma membrane. *Nature* **437**, 902-905.

Zhang, S. L., Yeromin, A. V., Zhang, X. H.-F., Yu, Y., Safrina, O., Penna, A., Roos, J., Stauderman, K. A. and Cahalan, M. D. (2006). Genome-wide RNAi screen of Ca2+ influx identifies genes that regulate Ca2+ release-activated Ca2+ channel activity. *Proc. Natl. Acad. Sci. USA* **103**, 9357-9362.

Zhou, Y., Meraner, P., Kwon, H. T., Machnes, D., Oh-hora, M., Zimmer, J., Huang, Y., Stura, A., Rao, A. and Hogan, P. G. (2010). STIM1 gates the store-operated calcium channel ORAI1 in vitro. *Nat. Struct. Mol. Biol.* **17**, 112-116.